Rare earth element composition of paleo-maar sediments (latest Pleistocene–Early Holocene), Jeju Island, Korea: Implications for Asian dust record and monsoon climate

Min Kyung Lee [a], Seung Hyoun Lee [b], Yong Il Lee [c, *], Ho Il Yoon [a], Kyu-Cheul Yoo [a]

[a] Korea Polar Research Institute, KIOST, Incheon 406-640, Republic of Korea
[b] Korea National Oil Corporation, Anyang, Gyeonggi-do, 431-711, Republic of Korea
[c] School of Earth and Environmental Sciences, Seoul National University, San 56-1 Sinlim-dong, Gwanak-gu, Seoul 151-747, Republic of Korea

A R T I C L E   I N F O

A B S T R A C T

The rare earth element (REE) composition of a 4.96 m-long sediment core retrieved from the Hanon paleo-maar in Jeju Island, Korea was studied to investigate the East Asian monsoon variations during the latest Pleistocene to early Holocene (22,300—9000 cal BP). The studied paleo-maar core sediment has two restricted source materials with distinctively different geochemical signatures: Asian dust blown from central Asia (especially northern China and Mongolia) and basement rock composed of trachybasalt. The REE characteristics of sediments depend on the relative contribution of these two sources and thus can be used to delineate the monsoon climate in Jeju Island. The proportion of Asian dust generally decreased gradually from 67% at 22,300 cal BP, indicative of progressive weakening of the winter monsoon strength in central Asia. Integration of the REE data with TOC and MS records reveals that the summer monsoon strength in Jeju Island decreased from 22,300 cal BP until the last glacial maximum at 18,000 cal BP, and then increased to 14,000 cal BP. The abrupt intensification of the summer monsoon occurred from 14,000 to 13,300 cal BP, followed by the weakened summer monsoon from 13,300 to 11,000 cal BP, in anti-phase with the strengthened winter monsoon in central Asia. In the early Holocene, Jeju Island experienced further intensified summer monsoon strength.

1. Introduction

Asian dust events have become an important environmental issue in East Asian countries such as China, Korea, and Japan, and their effects are also noticed in western North America across the North Pacific (Jaffe et al., 1999; Sun et al., 2001; VanCuren and Cahill, 2002; VanCuren, 2003; Zdanowicz et al., 2006; amongst others). Asian dust (called Hwangsa in Korea) occurs in nearly every spring. Major dustfall events are generally associated with strong northwesterly winds (Xiao et al., 1997; Zhang et al., 1997, 1999, Shao and Dong, 2006). Asian dust storms are known to cause harmful consequences to human life and health as well as an economic loss in the affected regions (Kwon et al., 2002; Yang et al., 2005; Batjargal et al., 2006; Zdanowicz et al., 2006; Hashizume et al., 2010). Asian dust events may have been more frequent and stronger during glacial periods than during interglacials due to

strengthening of the winter monsoons (Rea, 1994; Kohfeld and Harrison, 2003; Maher et al., 2010).

The pattern of climate in East Asia is dominated by the summer and winter monsoons. The East Asian monsoon is a dynamic interactive system that involves the ocean, land, and atmosphere. It is driven by the thermal difference between the Asian continent and the Pacific Ocean in the east and southeast (An et al., 1990). Summer monsoon carries a warm, moist, and maritime air onto the continent, and winter monsoon a cold and dry air out of north-central Asia where high pressure cell forms during the winter season.

The alternation of paleosols and loess units in the Loess Plateau of central China has been used as a proxy record of variations in the strength of the East Asian summer and winter monsoons over the past 2.5 million years (An et al., 1990, 1991; Ding et al., 1995; Liu and Ding, 1998; Sun et al., 2006). The surrounding ocean of East Asia, the North Pacific, has been influenced by East Asian monsoons (Windom, 1969). During the glacial periods when the climate was cold and dry, it is expected that the atmosphere was dusty, resulting in much dust fallout deposition in the downwind areas. In

Asian regions, significant amounts of airborne sediments from central or northern Asia are known to have been deposited in China (Pye and Zhou, 1989; An et al., 1990; 1991; Ding et al., 1995; Qiang et al., 2014), Korea (Mizota et al., 1991; Lim et al., 2005; Kim et al., 2012), and Japan (Xiao et al., 1999) as well as in the northern Pacific Ocean (Windom, 1969; Janecek and Rea, 1983, 1985; Rea et al., 1985; Pye and Zhou, 1989) during the Quaternary, mostly during the glacial periods in particular.

Using a paleo-maar sediment in Jeju Island the paleo-monsoonal climate changes during the latest Pleistocene to early Holocene were studied by Lee et al. (2008). They reported that Jeju Island experienced the coldest climate around 18,000 cal BP, and then there was an abrupt shift in climate regime from cold and arid to warm and humid conditions at around 14,000 cal BP, which represents the commencement of the last major deglaciation-like climate conditions. After this time, Jeju Island experienced the strong summer monsoon climate with two periods of the slightly weakened summer monsoon from 13,300 to 12,000 cal BP and from 10,500—9800 cal BP. This paleoclimate interpretation is consistent with that from a pollen record obtained from the same core sediment (Chung, 2007). Here, we report the rare earth element (REE) compositions of the same Jeju paleo-maar sediment for the same period during the latest Pleistocene to early Holocene. REEs are extremely insoluble in aqueous solutions, and therefore, tend to be transferred from source to sink without significant fractionation (Balashov et al., 1964; Nesbitt, 1979; Davies, 1980; Bierlein, 1995).

Jeju Island is the perfect place for studying the influence of Asian dust derived from dry areas in central Asia because of its downwind location (e.g., Lim et al., 2005) and simple geology comprising mostly of basaltic rocks. The REE characteristics of the paleo-maar sediments may depend on the relative contribution of two geochemically distinctive sources: the Asian dust transported from central Asia, especially northern China and Mongolia, and detritus derived from the catchment of the paleo-maar. The influx of the Asian dust depends on the climatic conditions of dust source regions: when the winter monsoon strengthens, more Asian dust becomes airborne and will be transported downwind. Conversely, when the summer monsoon is strengthened, it brings more precipitation to the region, resulting in stronger pedogenesis and less available airborne dust. In contrast to the dust source regions in central Asia, Jeju Island is located close to a moisture source and thus may not be sensitive to the changes in monsoon climate as much as is central China. The Asian dust influx to Jeju Island may faithfully follow the paleoclimatic conditions in central China as recorded in the Loess Plateau and caves in China, whereas the detrital influx from the catchment depends on the weathering states on Jeju Island. Any deviation of Jeju paleoclimate record from the paleo-monsoonal history recorded in the Loess Plateau and caves in China may indicate the difference in the characteristics of the monsoon climate between the two regions. By analyzing the REE characteristics of the paleo-maar sediment and combining them with the previous study results, this study aims to decipher the paleo-monsoon history of Jeju Island.

2. Environmental setting

The following environmental information is from Lee et al. (2008). The studied paleo-lake, Hanon paleo-maar, is located about 1 km west of Seoguipo in the southern part of Jeju Island, Korea (33°14′30″—33°15′00″N, 126°32′45″—126°33′15″E) (Fig. 1). Jeju Island is a shield volcano mostly composed of Quaternary trachyte and trachybasalt with minor welded tuff and the Quaternary Seoguipo Formation (Won, 1976; Lee, 1982) (Fig. 1). The study area is a paleo-maar formed by parasitic volcanism. It is filled with sediments and is now used as a rice field. The basement rock of the studied paleo-maar consists of trachybasalt. The studied paleo-
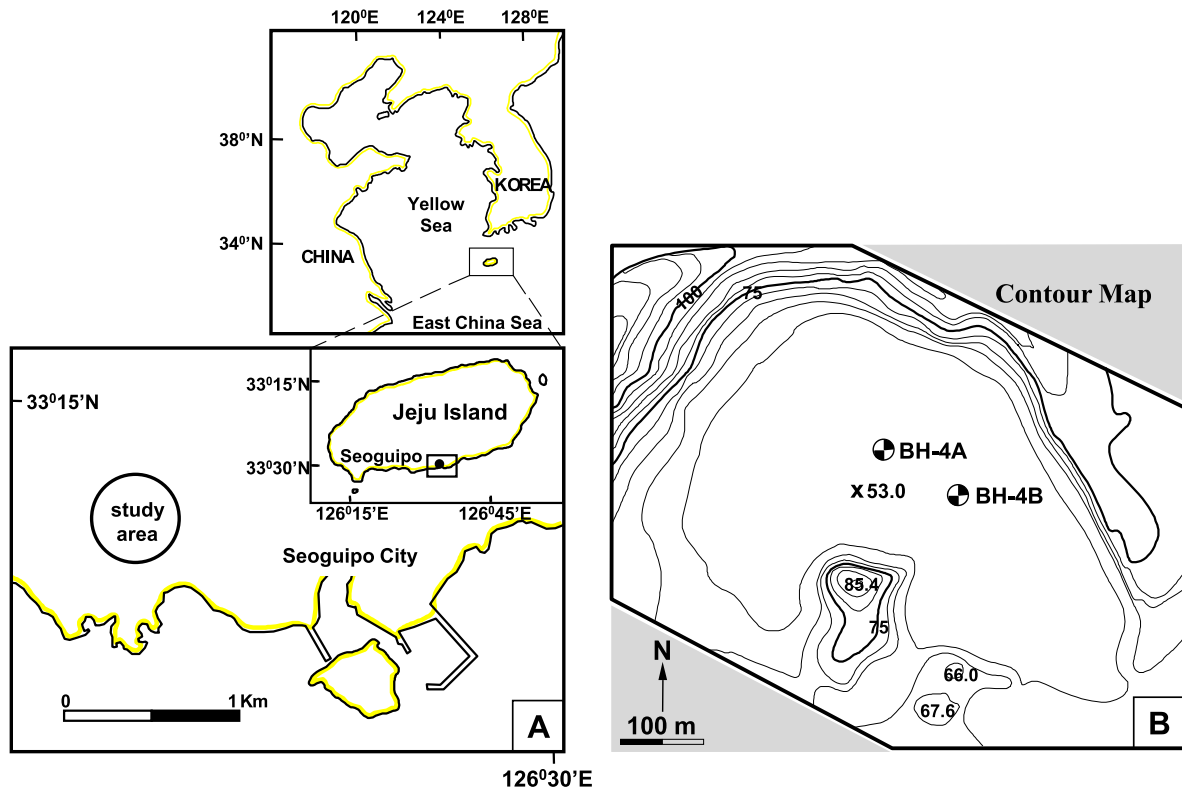

Fig. 1. (A) Location map of the study area. (B) Location of core BH-4B in the center of Hanon paleo-maar, Jeju Island (modified after Lee et al., 2008).

maar does not have prominent inlets and outlets, and it is an ellipsoidal basin that is 800 m long in the NW–SE direction and 500 m across in the NE–SW direction. The elevation difference between the basin surface and the surrounding hill is approximately 50 m (Fig. 1).

Jeju Island is currently located in the transition region between the temperate and subtropical zones. Geographically, it belongs to the eastern coast of the Eurasian continent and is adjacent to the West Pacific Ocean (Fig. 1). During winter, from December to January, it is cold and dry under the dominant influence of the Siberian high, whereas in summer, from June to August, it is hot and humid with frequent heavy rainfall. The mean annual precipitation during the three decades from 1971 to 2000 is approximately 1850 mm in the southern part of Jeju Island (Jeju Regional Meteorological Office; http://jeju.kma.go.kr). More than half of the annual precipitation falls during the summer season when a stationary front lingers across the Korean Peninsula for around a month. Winter precipitation is less than 10% of the annual total. The prevailing winds are southeasterly in summer and northwesterly in winter. In general, the latter are characterized by higher speed and stronger intensity.

3. Material and East Asian monsoon variations in Jeju Island

The detailed description of the studied BH-4B core (a 4.96 m long vibro core; Fig. 1) has been reported in Lee et al. (2008) and their study is summarized below (Fig. 2). The studied core is mainly composed of fine-grained sediments of clayey or silty mud and silt with less than 4% sand. The core sediment is interpreted to be composed of detritus derived from two different sources: detritus washed in from the surrounding volcanic hills and the eolian dust transported by winds from central Asia. The uppermost part (<60 cm) of the core sediments is considerably disturbed, which corresponds to the age interval from 6200 cal BP at the surface to 9000 cal BP at 60 cm from the core top. Sediments younger than 6000 cal BP were probably removed during cultivation. The age of bottom sediment of the core is estimated to be 22,300 cal BP. The core is divided into two intervals by the magnetic susceptibility (MS) value: the sediments at depths greater than 200 cm (corresponding to 14,000 cal BP) have high MS values (>30 × 10⁻⁵SI) with high-frequency and high-magnitude variations, and the highest value occurs at the depth of approximately 350 cm (corresponding to 18,000 cal BP), whereas the core sediments at depths less than 200 cm have very low MS values of less than 30 × 10⁻⁵SI, with low-frequency variations. Compared to trachybasalt in the crater rim of the paleo-maar, the MS values of Asian dust are low [600–1000 × 10⁻⁵SI (Lee et al., 2008) vs. <100 × 10⁻⁸SI (cf., Li et al., 2012; Wang et al., 2013)], and thus the MS values in the paleo-maar sediment may represent the weathering intensity of trachybasalt that controls the abundance of detrital magnetic minerals derived from the surrounding hills. This interpretation in turn suggests that the MS records can be used as an East Asian winter monsoon proxy. The total organic carbon (TOC) content of the core sediments ranges from 2.4 to 44 wt%, and the TOC content is anomalously high near the top of the core. The downcore variation in the TOC content shows that it abruptly changed at a depth of around 208 cm (corresponding to 14,400 cal BP). Below this depth, the TOC content is less than 6.5 wt%, whereas above this depth the TOC content has a range of 8.7–17 wt%. The lowest TOC value occurs at a depth of around 320 cm (corresponding to 17,700 cal BP). The MS and TOC records of the Hanon paleo-maar sediments reveal significant variations in the intensity of the winter and summer monsoons in Jeju Island, respectively, during the latest Pleistocene to early Holocene. Prior to around 21,300 cal BP, the summer monsoon was slightly stronger, even though the intensity of the summer monsoon was considerably weaker than that during the Holocene. The time interval from 21,300 to 14,000 cal BP represents the period with a very weak summer monsoon but very strong winter monsoon strength. At around 14,000 cal BP the summer monsoon began to strengthen, indicative of the timing corresponding to the onset of the last major deglaciation-like warming in Jeju Island. From the time of the last deglaciation-like warming to the early Holocene, the summer monsoon was weakened from 13,300 to 12,000 cal BP and from 11,500–9800 cal BP. Subsequently, the
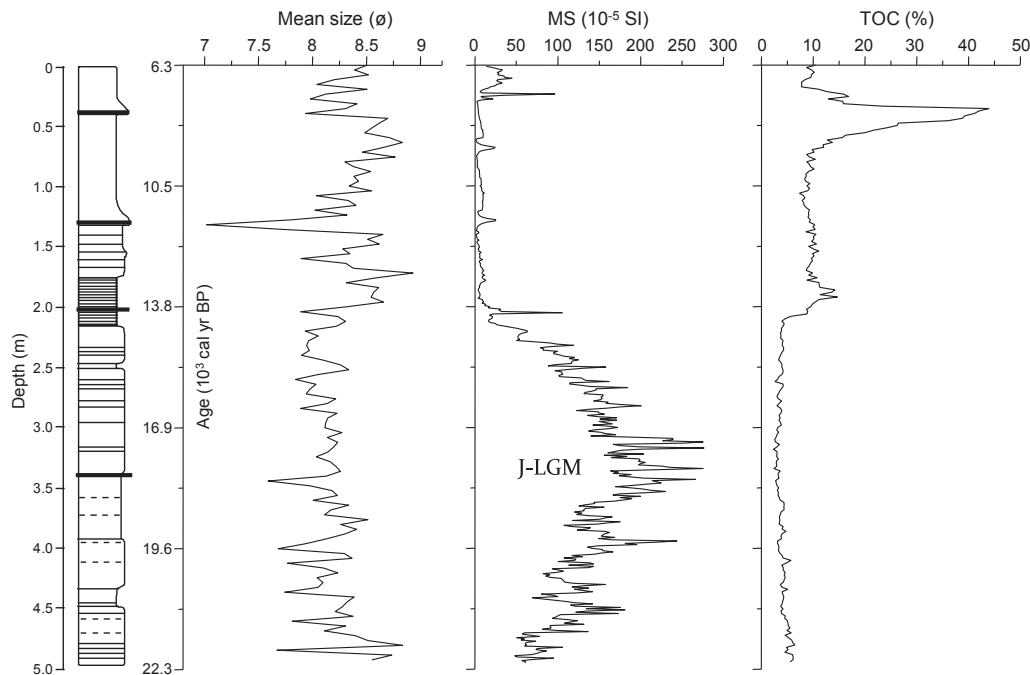

Fig. 2. The schematic columnar of core BH-4B with calibrated time markers and vertical variations of mean size, magnetic susceptibility, and total organic carbon (after Lee et al., 2008).

summer monsoon strengthened from 9800 cal BP. However, the winter monsoon did not strengthen during the same periods when the summer monsoon was weakened, suggestive of the weakening of the summer monsoon intensity does not necessarily indicate the strengthening of the winter monsoon.

4. Methods

The preparation of samples for REEs followed an acid digestion method and the procedure is as follows. The subsamples taken at 10 cm intervals were dried in an oven at 105 °C for two days. The dried samples were ground to less than 200-mesh powder using an agate mortar and the powdered samples were heated with 1 ml of 30% HCl in a sealed teflon bomb at 150 °C for 12 h. After adding each 1 ml of 48% Hf and 65% HNO_3 to dissolved solution, the mixed solution was heated at 150 °C for three days, and after reaction solution was dried completely on a hot plate. After cooling, the dried final residue was dissolved by adding 1 wt.% HNO_3 in 60 ml light-density polyethylene tube and the total weight of the redissolved solution was set to be 60 g. This solution was diluted to 1000-fold by adding 1 wt.% HNO_3 for REE analysis.

The composition of REE was analyzed for samples by using an Optima 3300 DV (Perkin−Elmer Sciex) inductively coupled plasma optical emission spectrometer (ICP-OES) at Korea Polar Research Institute. All the instrumental operating conditions of the ICP-OES are listed in Hur et al. (2003). Geochemical standards MAG-1 (USGS) and JA-2 (JSA) were analyzed for a measurement quality control. For comparison of sediment compositions, three basaltic basement rock samples from the surrounding rim were collected. Also used were Asian dust (Hwangsa) samples collected at Korea Meteorological Administration, Seoul on 21 March 2002 during the Asian dust event. Asian dust samples were collected on cellulose membrane filters using a high-volume air sampler. REE compositions of trachybasalt and Asian dust samples were also analyzed utilizing the same ICP-OES. Analytical precision for REE is generally better than 3%.

5. Results

The analytical results of REE compositions of core BH-4B sediments, trachybasalt, and Asian dust samples are given in Table 1. Total REE concentrations of core sediments show much variability ranging from 44 ppm to 321 ppm, and the condrite-normalized ratio of La/Yb [(La/Yb)$_N$] is also variable ranging from 3.4 to 14.0. The Eu/Eu* (where Eu/Eu* = Eu$_N$/[(Sm$_N$)(Gd$_N$)]$^{1/2}$, the subscript 'N' indicates normalized values) for core sediments varies from 0.77 to 0.97. The Eu/Eu* shows a gradual decrease of negative anomaly upcore (Fig. 3), and an abrupt increase with a small negative Eu anomaly is shown at 180, 200, 210, and 220 cm depths. A distinctive positive Ce anomaly (Ce/Ce*) (maximum 1.27) is observed at several horizons, at 200, 210, 220, and 390 cm depths.

Table 1
Rare earth elements concentrations in ppm for core BH-4B sediments, trachybasalt, and Asian dust sample.

Depth (cm)	La	Ce	Pr	Nd	Sm	Eu	Gd	Tb	Dy	Ho	Er	Yb	ΣREE	Eu/Eu[a]	Ce/Ce[a]	LaN/YbN
0	21.3	46.8	5.6	22.1	4.9	1.5	5.1	0.8	4.3	0.8	2.3	2.0	117.5	0.93	0.99	7.2
10	53.7	95.5	12.0	45.3	8.9	2.6	9.2	1.3	6.7	1.2	3.2	2.6	242.2	0.89	0.83	14.0
20	38.7	75.7	9.1	35.4	7.0	2.0	7.0	1.0	5.2	0.9	2.6	2.1	186.8	0.90	0.90	12.2
30	23.3	52.1	5.6	21.6	4.5	1.4	4.6	0.7	3.8	0.7	2.0	1.7	121.9	0.92	1.03	9.3
40	13.3	26.6	3.1	12.2	2.5	0.7	2.5	0.4	2.0	0.4	1.1	0.9	65.5	0.89	0.92	10.3
50	26.0	50.5	6.0	22.8	4.7	1.4	4.6	0.6	3.6	0.6	1.8	1.5	124.3	0.90	0.90	11.7
60	31.9	61.5	7.4	28.1	5.6	1.7	5.7	0.8	4.3	0.8	2.2	1.8	151.6	0.92	0.89	12.1
70	22.2	45.9	5.5	21.2	4.3	1.2	4.2	0.6	3.2	0.6	1.7	1.4	111.9	0.90	0.94	10.3
80	29.2	59.3	7.2	27.2	5.4	1.6	5.3	0.7	4.1	0.7	2.0	1.8	144.5	0.89	0.93	11.0
90	10.4	24.1	3.0	12.2	2.6	0.7	2.3	0.3	1.9	0.3	1.0	0.9	59.8	0.92	1.01	7.7
100	29.8	59.8	7.1	27.5	5.7	1.7	5.8	0.8	4.6	0.9	2.4	2.0	148.1	0.91	0.92	9.9
110	46.4	91.2	11.1	42.4	8.4	2.3	8.3	1.2	6.2	1.1	3.1	2.5	224.3	0.84	0.91	12.3
120	42.9	84.3	10.3	38.6	7.6	2.1	7.8	1.1	5.7	1.0	2.8	2.4	206.5	0.84	0.91	12.2
130	44.3	86.3	10.4	39.6	7.8	2.2	7.8	1.1	5.7	1.0	2.8	2.3	211.2	0.86	0.90	12.9
140	44.2	86.4	10.4	40.0	8.1	2.2	8.1	1.1	6.1	1.1	3.0	2.5	213.2	0.84	0.90	11.8
150	43.1	82.4	10.1	38.2	7.5	2.1	7.5	1.1	5.8	1.0	2.9	2.5	204.1	0.86	0.89	11.7
160	42.7	82.6	10.1	38.2	7.6	2.1	7.7	1.1	5.7	1.0	2.8	2.3	203.9	0.85	0.90	12.2
170	42.4	83.4	10.1	37.8	7.3	2.0	7.5	1.0	5.4	0.9	2.7	2.2	202.7	0.83	0.91	12.7
180	11.4	28.1	3.5	14.4	3.3	1.0	3.4	0.5	3.0	0.6	1.6	1.4	72.3	0.90	1.06	5.3
190	41.7	80.5	9.7	36.6	7.2	2.0	7.5	1.0	5.4	0.9	2.7	2.2	197.4	0.83	0.89	12.7
200	6.3	18.1	1.8	8.0	1.9	0.6	2.0	0.3	2.1	0.4	1.3	1.2	43.9	0.92	1.24	3.4
210	9.2	27.1	2.6	11.4	2.7	0.8	2.7	0.4	2.6	0.5	1.4	1.4	62.9	0.91	1.27	4.5
220	6.5	18.3	1.7	7.7	1.9	0.6	2.0	0.3	2.0	0.4	1.2	1.1	43.6	0.97	1.23	4.0
230	58.9	116.7	13.0	49.4	9.8	2.6	9.7	1.3	7.2	1.3	3.5	3.0	276.4	0.81	0.93	13.1
240	61.7	129.6	14.2	52.7	10.3	2.8	10.5	1.4	7.5	1.3	3.8	3.3	299.2	0.82	0.98	12.6
250	56.8	118.7	13.0	49.0	9.7	2.6	9.9	1.3	7.2	1.3	3.6	3.1	276.1	0.83	0.97	12.4
260	23.8	59.2	6.0	24.5	5.4	1.6	5.6	0.9	4.8	0.9	2.7	2.4	137.7	0.88	1.12	6.6
270	38.0	80.3	9.2	36.4	7.5	2.0	7.5	1.1	5.9	1.1	3.1	2.7	194.7	0.83	0.97	9.5
280	27.4	59.7	6.8	27.4	5.8	1.6	6.0	0.9	5.1	1.0	2.7	2.5	147.0	0.85	0.98	7.4
290	54.7	118.0	12.4	47.1	9.2	2.5	9.3	1.3	6.8	1.2	3.5	3.0	268.9	0.81	1.00	12.1
300	27.4	59.6	7.0	28.7	6.2	1.7	6.2	0.9	5.2	1.0	2.8	2.5	149.3	0.85	0.98	7.2
310	65.9	136.7	15.3	57.7	11.4	3.2	11.8	1.6	8.4	1.5	4.1	3.5	321.1	0.84	0.96	12.6
320	57.8	119.8	13.8	52.2	10.2	2.7	10.4	1.4	7.5	1.3	3.8	3.2	284.0	0.82	0.96	12.1
330	21.4	52.6	5.8	24.0	5.3	1.5	5.4	0.8	4.7	0.9	2.5	2.2	127.3	0.89	1.08	6.4
340	64.1	131.6	14.8	55.8	11.0	3.0	11.2	1.5	7.9	1.4	3.9	3.3	309.3	0.83	0.96	12.9
350	66.0	136.3	14.9	56.6	11.0	3.0	11.3	1.5	7.9	1.4	3.9	3.3	317.0	0.82	0.96	13.5
360	53.2	111.4	12.2	46.1	8.9	2.3	9.1	1.2	6.5	1.2	3.3	2.8	258.2	0.80	0.97	12.5
370	57.0	117.0	13.0	49.6	9.7	2.5	9.8	1.3	6.9	1.2	3.4	2.9	274.5	0.80	0.95	13.1
380	55.0	113.8	12.5	46.6	9.1	2.4	9.2	1.3	6.6	1.2	3.3	2.9	263.8	0.81	0.97	12.8
390	26.0	71.5	6.1	24.0	5.1	1.4	5.4	0.8	4.3	0.8	2.3	2.1	149.8	0.84	1.26	8.2

Table 1 (*continued*)

Depth (cm)	La	Ce	Pr	Nd	Sm	Eu	Gd	Tb	Dy	Ho	Er	Yb	ΣREE	Eu/Eu[a]	Ce/Ce[a]	LaN/YbN
400	53.0	109.1	12.1	46.1	8.9	2.4	9.3	1.2	6.5	1.2	3.3	2.7	255.6	0.82	0.96	13.2
410	52.8	109.8	12.0	45.8	8.9	2.3	9.2	1.2	6.5	1.1	3.2	2.8	255.6	0.78	0.97	12.8
420	46.2	93.9	9.5	35.5	6.9	1.8	7.3	1.0	5.1	0.9	2.6	2.3	213.0	0.79	0.97	13.4
430	22.3	54.2	5.4	21.8	4.7	1.3	4.8	0.7	4.0	0.7	2.2	2.0	124.2	0.85	1.10	7.5
440	44.1	82.6	8.9	33.2	6.4	1.6	6.5	0.9	4.7	0.8	2.4	2.1	194.3	0.79	0.89	14.0
450	46.8	91.0	9.8	36.6	7.1	1.9	7.3	1.0	5.3	1.0	2.7	2.4	212.8	0.82	0.92	13.1
460	40.3	80.2	8.6	32.5	6.4	1.6	6.5	0.9	4.9	0.9	2.5	2.3	187.7	0.78	0.94	11.9
470	40.5	78.5	8.5	32.2	6.4	1.7	6.4	0.9	4.8	0.9	2.4	2.2	185.2	0.80	0.92	12.5
480	44.7	90.5	10.3	38.4	7.4	1.8	7.5	1.0	5.2	0.9	2.6	2.3	212.6	0.77	0.94	13.2
490	43.7	85.4	9.8	36.9	7.1	1.8	7.4	1.0	5.5	1.0	2.8	2.4	204.9	0.77	0.91	12.1
Trachy-basalt[a]	67.5	119.0	15.6	61.3	12.5	4.2	14.1	2.0	9.9	1.8	4.7	3.6	316.2	0.97	0.81	12.4
Asian dust[b]	41.2	86.9	10.0	37.4	7.1	1.5	7.1	1.0	5.4	1.0	3.1	2.8	204.6	0.67	0.97	9.7

[a] Average of three samples.
[b] Collected on March 21, 2002 in Seoul.

The abundance of REE in the trachybasalt and Asian dust samples has different values with 316 ppm and 205 ppm, respectively. Chondrite-normalized patterns are significantly different (Fig. 4A). Trachybasalt is characterized by LREE-enriched patterns with fractionated HREE (Gd/Yb = 3.1) and negligible Eu anomaly (Eu/Eu* = 0.97). In contrast, the Asian dust sample is characterized by fractionated LREE patterns with relatively flat HREE (Gd/Yb = 2.0) and a pronounced negative Eu anomaly (Eu/Eu* = 0.67). Trachybasalt shows a slightly negative Ce anomaly (Ce/Ce* = 0.81), but the Asian dust sample does not have a Ce anomaly (Ce/Ce* = 0.97).

6. Discussion

6.1. Rare earth elements distribution

Based on the chondrite-normalized REE patterns and Eu anomaly, the REE distribution patterns of core sediments are subdivided into six types (Fig. 5). Type I REE pattern is very similar to the Asian dust REE pattern. The chondrite-normalized ratio of Eu/Eu* and Ce/Ce* for the type 1 REE pattern ranges from 0.77 to 0.82 and 0.89 to 0.97, respectively, showing that the Eu/Eu* is smaller than that of the Asian dust. (La/Yb)$_N$ and (Gd/Yb)$_N$ ratios range from 11.87 to 14.00 and 2.29 to 2.63, respectively. HREE is more fractionated than that of Asian dust. The type 1 REE pattern occurs in the lowermost part of core sediments at 420, 440, 450, 460, 470, 480, and 490 cm depths.

Type 2 REE pattern is generally similar to that of type 1, but shows enriched REE concentration than that of the latter. The chondrite-normalized ratios of (La/Yb)$_N$ and (Gd/Yb)$_N$ range from 12.15 to 13.25 and from 2.47 to 2.76, respectively. The Eu/Eu* for the type 2 REE pattern ranges from 0.78 to 0.82, indicating that Eu/Eu* is very similar to that of the type 1. The type 2 REE pattern is observed in sediments at 290, 360, 370, 380, 400, and 410 cm depths.
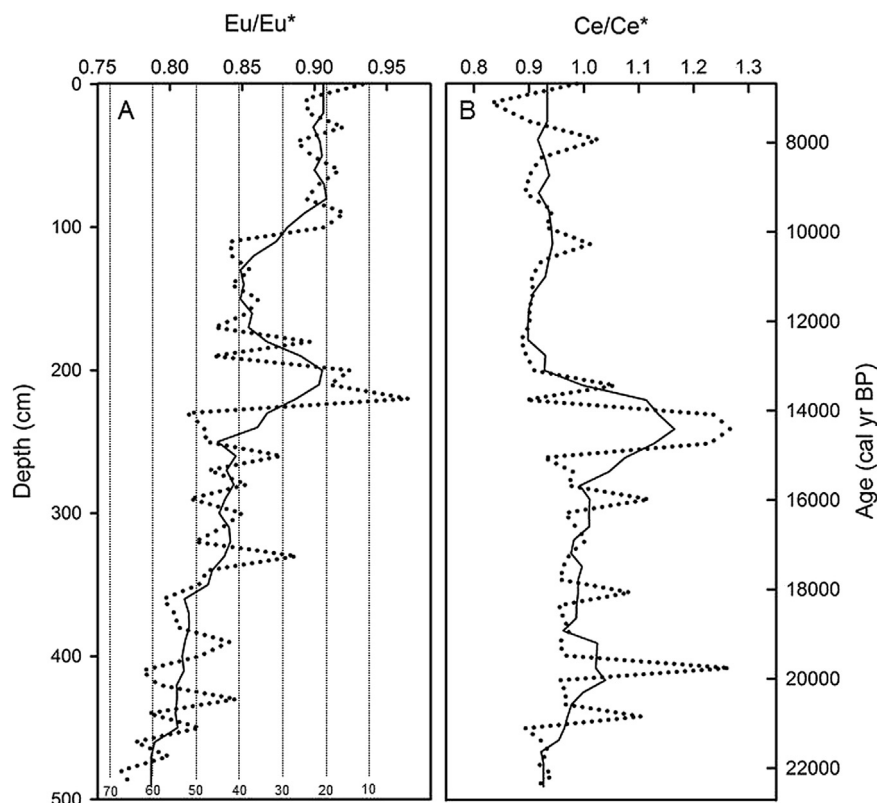

Fig. 3. Vertical variations of Eu anomaly (Eu/Eu*) and Ce anomaly (Ce/Ce*) of core BH-4B, Jeju Island. Vertical dotted lines with numbers at the bottom in (A) represent the proportion of the Asian dust calculated by using an Eu anomaly.
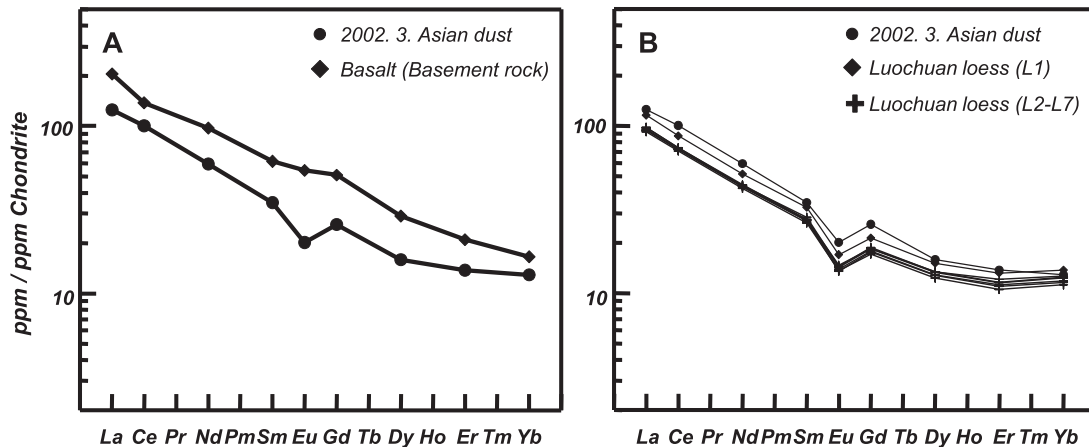
Fig. 4. (A) The chondrite-normalized REE patterns of trachybasalt surrounding the paleo-maar and the Asian dust samples collected in Seoul, Korea on March 21, 2002. (B) The chondrite-normalized REE patterns of Luochuan loess in China back to 800 ka (Gallet et al., 1996). The chondrite-normalized REE pattern of the Asian dust sample is very similar to those of Luochuan loess.

The $(La/Yb)_N$ of type 3 ranges from 6.38 to 8.23, displaying very flat REE patterns than those of types 1 and 2 having $(La/Yb)_N$ ratios more than 10. The Eu/Eu* ranges from 0.84 to 0.89, and thus has a weaker negative Eu anomaly than that of types 1 and 2. The type 3 REE pattern is observed in sediments at 260, 280, 300, 330, 390, and 430 cm depths. The type 3 shows a strong positive Ce anomaly with the chondrite-normalized ratio of Ce/Ce* ranging from 0.98 to 1.26. The sample at 390 cm depth shows a very strong positive Ce anomaly, 1.26.

Type 4 REE pattern is similar to that of types 1 and 2. The Eu/Eu* ranges from 0.81 to 0.86, and thus the type 4 has a slightly more negative Eu anomaly than that of type 3 but weaker than that of type 1. Type 4 is divided into two subgroups on the basis of the total REE concentration, one with relatively enriched total REE concentration occurring in the deeper part below 2 m depth (type 4a) and the other with relatively less enriched total REE occurring in the shallower part (type 4b) except for a sample at 270 cm depth. The type 4a shows slightly higher Eu/Eu* ratios and occurs in sediments at 230, 240, 250, 310, 320, 340, and 350 cm depths and the type 4b is observed in sediments at 110, 120, 130, 140, 150, 160, 170, 190, and 270 cm depths.

Type 5 REE pattern occurs in the most upper part of core sediments and shows a similar pattern to that of trachybasalt. However, total REE concentrations for the type 5 are depleted, ranging from 60 to 242 ppm, less than that of trachybasalt (316 ppm). The Eu/Eu* and Ce/Ce* for the type 5 range from 0.89 to 0.93 and 0.83 to 1.03, respectively and thus, the type 5 shows a very weak negative Eu anomaly close to that of trachybasalt. Even though the $(La/Yb)_N$ ranges from 7.18 to 14.01, the REE pattern of the type 5 shows the same fractionated pattern to that of trachybasalt. The type 5 pattern occurs in sediments of core top to 100 cm depth interval.

Type 6 REE pattern, occurring in samples at 180, 200, 210, and 220 cm depths, shows a very different REE pattern from those of other core sediments, Asian dust, and trachybasalt. The Eu/Eu* ranges from 0.90 to 0.97, showing the weakest negative Eu anomaly, almost identical to that of trachybasalt, but total REE concentrations are much depleted. The REE pattern of the type 6 is the most flattened among all samples, with the $(La/Yb)_N$ ranging from 3.39 to 5.29. The Ce/Ce* ranges from 1.06 to 1.27, representing the strongest positive Ce anomaly.

6.2. Asian dust influence

The Eu/Eu* time-series spanning the latest Quaternary to early Holocene are characterized by high-frequency, high-amplitude variations (Fig. 3). The comparison of the Eu/Eu* curve with paleo-monsoon proxy records from the Loess Plateau and caves in China is shown in Fig. 6. Whereas the Eu/Eu* curve (Fig. 6B) generally resembles the quartz grain-size profile in the Chinese Loess Plateau at Luochuan (a winter monsoon record) (Fig. 6A; Xiao et al., 1995), in detail the basic data display slightly different variability at ~15,000 cal BP and in the time interval from ~14,000 to 11,000 cal BP, and the variation in the latter interval is more similar to that observed from oxygen-isotope records of stalagmites from Sanbao cave in China (a summer monsoon record) (Fig. 6C; Wang et al., 2008).

The studied paleo-maar sediment has two restricted terrestrial source materials: (1) basement rock composed of trachybasalt and (2) Asian dust blown from central Asia. Geochemical characteristics (REE, Th, U, and La/Th) of loess reveal that the Chinese Loess Plateau, the Luochuan loess as a representative, was derived from well-mixed sedimentary protoliths which underwent numerous upper-crustal recycling processes (Gallet et al., 1996). They reported REE compositions of the Luochuan loess back to 800 ka, displaying highly uniform REE patterns (except for Ce) characterized by the upper continental crust (UCC) ratios: $(La/Yb)_N = 10$ and $Eu/Eu* = 0.66$ (Fig. 4B). The REE of the Asian dust samples in this study shows $(La/Yb)_N = 9.71$ and $Eu/Eu* = 0.67$, being almost identical to that of the Luochuan loess. The REE characteristics of Asian dust analyzed in this study are also very similar to those of present-day Asian dust in other studies (e.g., Ryu et al., 2007; Yang et al., 2007). This indicates that chemical properties of Asian dust per se that has been transported from central Asia to the Korean Peninsula might have been nearly consistent for at least 800,000 years, although it is difficult to establish considering the opinion that during the glacials the Yellow Sea basin was exposed and served as a major dust source to Korea (e.g., Kim et al., 2012). The chondrite-normalized REE pattern of basement rock, trachybasalt, of the studied lake shows Eu-enriched REE pattern ($Eu/Eu* = 0.97$), which is identical to geochemical characteristics of basalt reported by McLennan et al. (1993).

The profile of Eu/Eu* shows a gradual decrease of negative Eu anomaly up core (Fig. 3), indicating a gradual decrease of Asian dust input to the studied paleo-maar, probably because of gradual weakening of winter monsoons. If Eu anomalies of the studied paleo-maar sediments resulted from simple mixing between Asian dust and trachybasalt-derived detritus without geochemical fractionation, the proportion of the Asian dust input from central Asia to Jeju Island can be inferred. Using a binary mixing model with Eu/
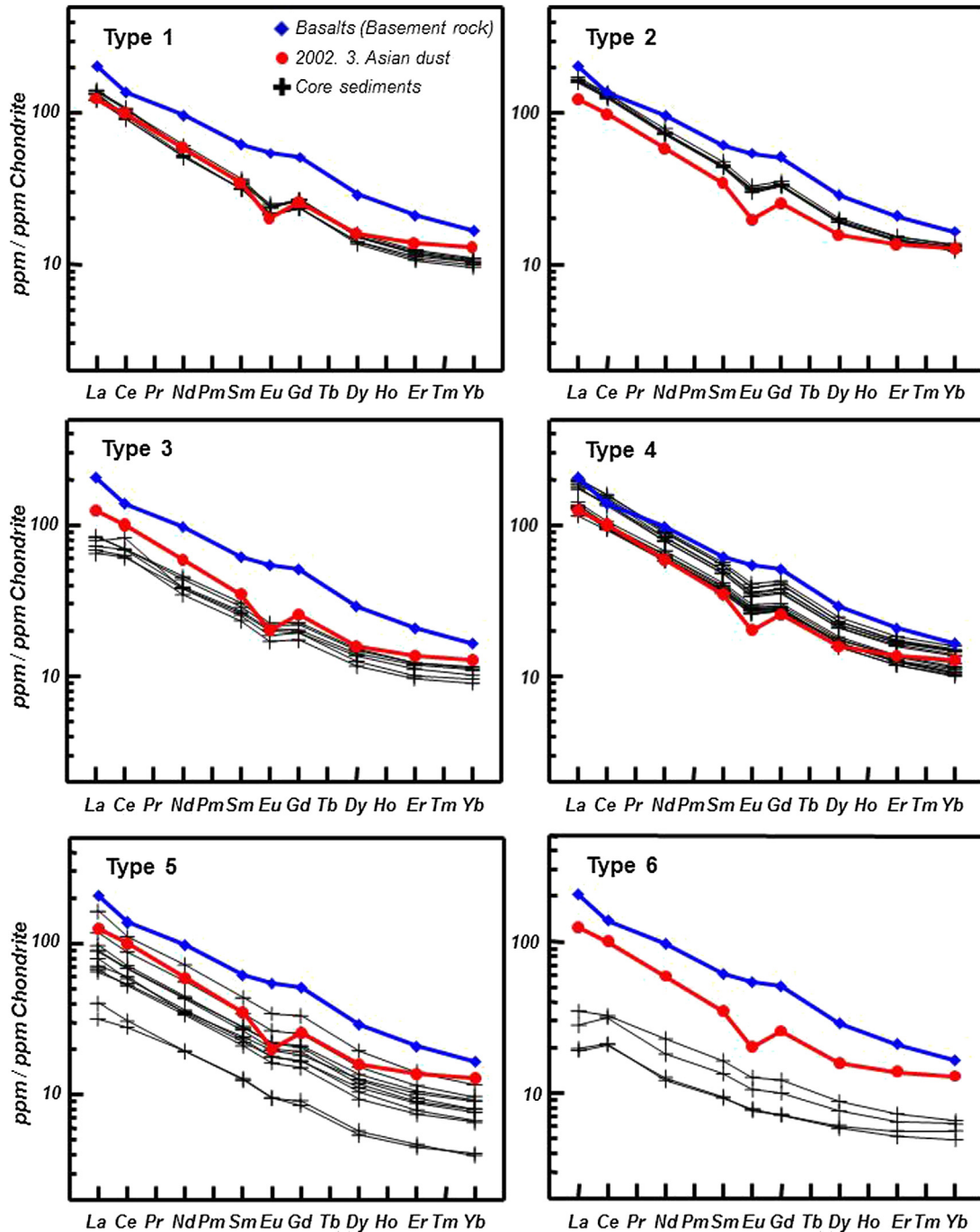
Fig. 5. The six REE patterns of core BH-4B sediments base on the chondrite-normalized REE patterns and Eu anomaly.

Eu* end values of 0.97 for trachybasalt and 0.67 for Asian dust from central Asia, the contribution of the Asian dust was estimated to be up to 67% during the last glacial period and varies down to nil. The results of calculation reveal that the Asian dust proportion ranges from 27 to 67% during the last glacial period and from 13 to 43% during the Holocene (Fig. 3). Such large Asian dust flux during the last glacial period is in agreement with the results of other studies. Xiao et al. (1999) reported that the Asian quartz flux in Lake Biwa, Japan was three to five fold more than the fluvial quartz flux during the glacial periods. Windom (1969) suggested that up to 75% of the nonbiogenic component of North Pacific deep-sea sediment was atmospheric dust fallout during the glacial periods. Kohfeld and

Harrison (2003) reported that the mass accumulation rate for MIS 2 was 2.1 times greater than that for MIS 1 on the Chinese Loess Plateau.

The vertical variation of Eu/Eu* indicates that the Asian dust flux associated with winter monsoon intensity fluctuated with high magnitude during the glacial period than in the Holocene. The REE distribution patterns of paleo-maar sediments before ca. 20,500 cal BP are dominated by type 1 with the proportion of the Asian dust ranging from 50 to 67%. From 20,500 to ca. 15,000 cal BP, the paleo-maar sediments are represented by the REE patterns of types 2, 3, and 4a, and these types alternate during this time period. During this period the Asian dust comprises 27–63% of the
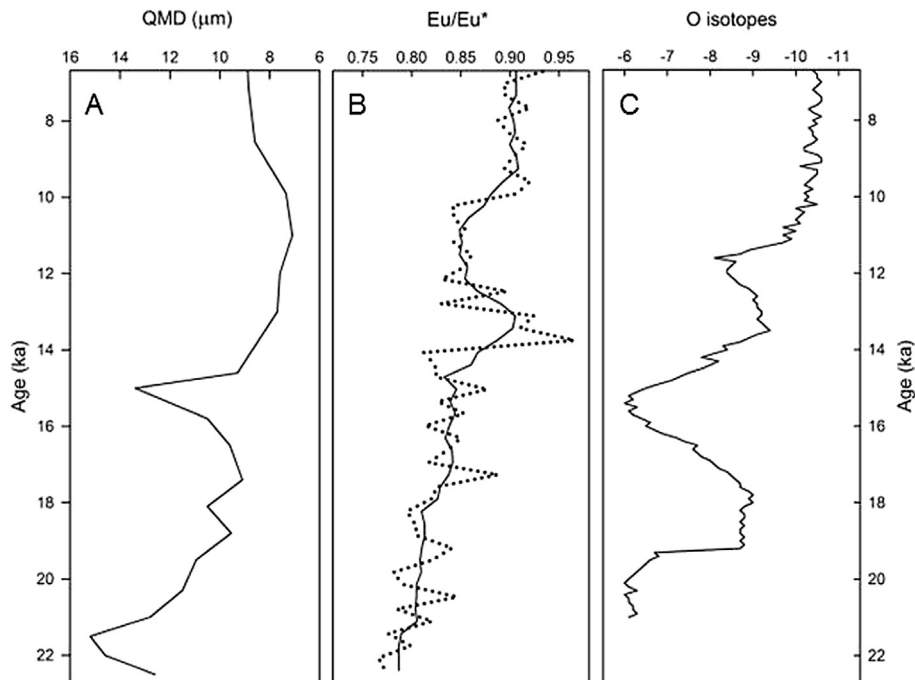
Fig. 6. Comparison of (B) Eu/Eu* of core BH-4B sediments with (A) quartz median diameter of the Chinese Loess Plateau (a winter monsoon record)(Xiao et al., 1995) and (C) oxygen-isotope records of stalagmites from Sanbao cave in China (a summer monsoon record) (Wang et al., 2008).

sediment: 50–63% (type 2), 27–43% (type 3), and 43–53% (type 4a), reflecting a variability of the winter monsoon intensity. Although the winter monsoon was strong at about 15,000 BP in the Chinese Loess Plateau record (Fig. 6A), it is not apparent in the Jeju record. At ca. 14,500 cal BP, the REE distribution pattern (type 6) is very different from those of Asian dust and trachybasalt, and has very low total REE concentrations, but the Eu/Eu* value of the type 6 is similar to that of trachybasalt (Fig. 5). The proportion of the Asian dust ranges from nil to 23%. This observation can be accounted for by the rapid increase of detrital input from highly weathered trachybasalt, probably due to abundant precipitation, and dilution effect by high organic material as evidenced by high TOC content (Fig. 2). From 13,000 cal BP to 11,000 cal BP the type 4b REE pattern occurred with increased Asian dust input (37–47%) by a factor of two to that of the type 6 REE pattern in the immediately preceding time interval. This time interval seems to be represented by the increased strength of the winter monsoon in central Asia.

Interestingly, the Asian dust record during 14,300–13,300 cal BP and during 13,300–11,000 cal BP resembles the Bolling-Allerod (BA) and Younger Dryas (YD) features observed in Hulu and San-bao caves in China (Fig. 6), suggestive of relatively strong and weak summer monsoon intensities, respectively (Wang et al., 2001, 2008). However, the stalagmite oxygen-isotope record is inter-preted as a proxy indicator of a vapor source or track, rather than that of monsoon precipitation (Pausata et al., 2011). Considering dating errors and resolution difference, the Eu/Eu* data suggest that the BA can be correlated with the type 6 REE pattern and the YD with the type 4b pattern. The possible connection of the central Asian winter monsoon events recorded in Jeju Island with the BA and YD features of north polar regions is worthy of note and needs further investigation.

The early Holocene is characterized by the type 5 pattern, and both REE pattern and Eu/Eu* values are close to those of trachy-basalt. The average mixing ratio of Asian dust to the studied paleo-maar sediment was about 22% and consistent (16.7–26.7% range), suggestive of weak winter monsoons.

6.3. Paleo-monsoon climate in Jeju Island

As described above, the Eu/Eu* record shows that the input of Asian dust reached its highest proportion (67%) in the core bottom sediment and its contribution generally decreased until the time of the last glacial maximum in Jeju Island (J-LGM). The TOC (a summer monsoon proxy) and MS (a winter monsoon proxy) records reveal that Jeju Island experienced the coldest time at about 18,000 cal BP (Lee et al., 2008). The record of Asian dust flux represents the paleoclimate change of Asian dust source regions in central Asia. The Eu/Eu* record of the studied paleo-maar sediments indicates that winter monsoon was very strong in central Asia prior to 18,500 cal BP, during which central Asia was very arid enough to supply abundant Asian dust. Xiao et al. (1995) reported that quartz median diameter (Q_{MD}) and quartz maximum diameter (Q_{max}) of the Luochuan loess-paleosol sequence, the proxy records for winter monsoon strength, reached their maximum value at 21,500 BP (Fig. 6A), and the onset of deglacial warming is interpreted to have occurred at ~19,000 BP (Peterse et al., 2011). Lee et al. (2008) pointed out that the timing of the LGM in the Chinese Loess Plateau was slightly earlier (2000–3000 y) than that in Jeju Island. Wu et al. (2002) suggested that changes in the temperature (responsible for wind intensity) and precipitation (responsible for extent of dust source area) in the Chinese Loess Plateau were not in phase during the last 30 ka: the coldest temperature occurred around 2000–3000 y prior to the precipitation minimum event. This idea was adopted when explaining the peak aeolian quartz flux in the Lake Biwa sediments in Japan (Xiao et al., 1999). If this were the case in central Asia, we would expect an increasing proportion of the Asian dust until the J-LGM in our paleo-maar sediment. However, the Asian dust flux did not increase as expected. Thus, this explanation does not hold true for the record in Jeju Island. Alternatively, the increased input of trachybasalt-derived detritus may be responsible for the decreasing trend of Asian dust influence, suggesting that Jeju Island was under the relatively strong influence of summer monsoons. Lee et al. (2008) interpreted the maximum

MS at around 18,000 cal BP as the timing of the strongest winter monsoon coupled with a very weak summer monsoon. Although it was interpreted that Jeju Island experienced the coldest temperature during the J-LGM (Lee et al., 2008), the difference in the modeled temperatures of Jeju Island between the LGM in central China (21–18 ka) and middle Holocene is estimated to be less than 3C° (Lu et al., 2013), suggesting that temperature influence was not significant. Rather, Jeju Island was under the progressively weakening summer monsoon strength from 22,300 cal BP onwards. At the time of the J-LGM, Jeju Island witnessed the largest input of primary inherited magnetic components (maximum MS) from the most weakly weathered soils of basalt (cf. Lu et al., 2008), probably due to the maximum reduction of summer monsoon strength. This interpretation suggests that until the J-LGM the weakening of the summer monsoon strength in Jeju Island was in phase with the weakening of the winter monsoon strength in central Asia. However, during this period of weakening summer monsoon strength there were three somewhat wet time intervals between 22,300 and 18,500 cal BP punctuated by two short dry times as indicated by the MS data (Fig. 3). Accordingly, the Eu/Eu* record reveals that the J-LGM was not the timing of the coldest and maximum winter monsoon strength, but the timing of the weakest summer monsoon strength in Jeju Island. After the highest MS value at ~18,000 cal BP, the MS value gradually decreased until ~14,000 cal BP, and during this time interval the proportion of Asian dust fluctuated between 30 and 53%. As weathering of basalt increases, the primary ferromagnetic mineral is known to weather directly to an antiferromagnetic mineral (hematite and/or goethite) (Lu et al., 2008). Thus, such a decreasing MS trend from 18,000 cal BP to 14,000 cal BP may represent a possible progressive increase in removal of magnetic components during pedogeneic development under increasing summer monsoon intensity.

During ~14,500 to ~13,300 cal BP, the proportion of Asian dust drastically decreased to almost nil to 23%, and this time interval is coeval with the onset of the major last deglaciation-like warming in Jeju Island as noted by the rapid increase in TOC content (Lee et al., 2008). During this interval, Jeju Island seems to have experienced significantly intensified summer monsoon strength. Dramatic increase of precipitation might have induced increased soil development and enhanced land-plant productivity (cf., Feng et al., 2002), which resulted in the deposition of detritus from highly weathered trachybasalt and land-plant debris in the paleo-maar, as indicated by high TOC content (Fig. 2), predominately organic matter of terrestrial origin (Lee et al., 2008). Subsequently, Jeju Island experienced the weakened summer monsoon intensity from ~13,000 to 11,000 cal BP, indicated by the slightly reduced TOC content and increased Asian dust proportion. Lee et al. (2008) pointed out that there were two weakening events of summer monsoon intensity in Jeju Island from the last deglaciation-like warming to the early Holocene, the timing of these two events being similar to the YD event. The similar weakening event of the summer monsoon strength (YD) was also reported from the Yangtze River delta in China (Yi et al., 2003). Then, the intensity of the summer monsoon became strong in the early Holocene, representing the weakening of eolian activity (cf., Qiang et al., 2014). Most of the sediments deposited during the latest glacial period were deposited under an oxic state as represented by a non- to positive Ce anomaly (cf., Wright et al., 1987; Wilde et al., 1996), whereas the early Holocene sediments were deposited under a slightly less oxic state.

In summary, the schematic presentation of the Jeju Island summer monsoon climate is depicted in Fig. 7. From 22,300 cal BP to the J-LGM the central Asian winter and the Juju Island summer monsoon changes covaried, both toward the weakening intensity, whereas from the J-LGM to the early Holocene they show an inverse
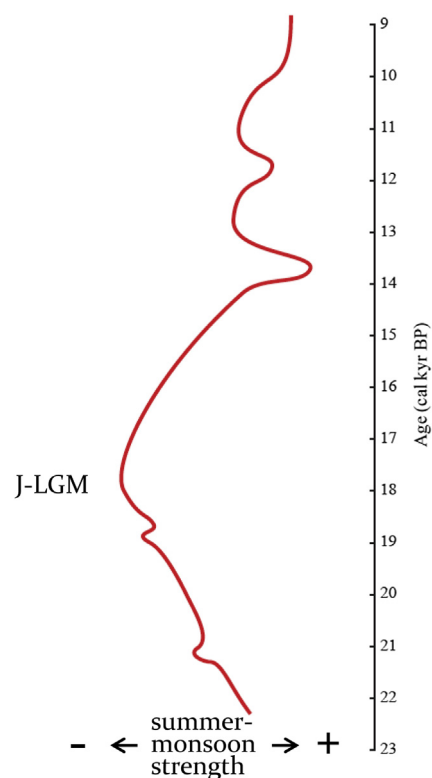

Fig. 7. The schematic presentation of variations of the summer monsoon strength recorded in Jeju Island on the basis of integration of REE, MS, and TOC data.

behavior between intensifying summer monsoon in Jeju Island and weakening winter monsoon strength in central Asia (Fig. 6).

7. Conclusions

1. The REE characteristics of the Hanon paleo-maar sediments in Jeju Island, Korea represent variations of the relative contribution of two geochemically distinctive sources: the Asian dust transported from central Asia and detritus derived from trachybasalt surrounding the paleo-maar. From 22,300 to 9000 cal BP the REE record reveals that due to its location close to the moisture source the monsoon climate of Jeju Island was mainly dominated by changes of the summer monsoon strength. During this period the winter monsoon strength in central Asia became progressively weakened.

2. Integration of the REE results with the MS and TOC data of Lee et al. (2008) shows that from 22,300 cal BP, the intensity of the summer monsoon strength was decreased progressively until 18,000 cal BP (J-LGM) when the summer monsoon strength was the weakest. Then, the summer monsoon strength became progressively intensified until 14,000 cal BP when the abrupt strong intensification occurred. The strong summer monsoons lasted until 13,300 cal BP. The winter monsoon strength in central Asia became weakened during this interval. From 13,300 cal BP to 11,000 cal BP the summer monsoon was weakened in anti-phase with the strengthened winter monsoon in central Asia. In the early Holocene, Jeju Island experienced further strengthened summer monsoons.

figures. This manuscript has benefitted from helpful comments by two anonymous journal reviewers.

Appendix A. Supplementary data

Supplementary data related to this article can be found at http://dx.doi.org/10.1016/j.quaint.2014.05.036.

References

An, Z.S., Liu, T.S., Lu, Y.C., Porter, S.C., Kukla, G.J., Wu, X.H., Hua, Y.M., 1990. The long-term paleomonsoon variation recorded by the loess-paleosol sequence in central China. Quaternary International 7/8, 91—95.

An, Z.S., Kukla, G.J., Proter, S.C., Xiao, J.L., 1991. Evidence of monsoon variation on the Loess Plateau of central China during the last 130,000 years. Quaternary Research 36, 29—36.

Balashov, Y.A., Ronov, A.B., Migdisov, A.A., Turanskaya, N.V., 1964. The effect of climate and facies environment on the fractionation of the rare earth elements during sedimentation. Geochemistry International 1, 951—969.

Batjargal, Z., Dulam, J., Chung, Y.S., 2006. Dust storms are an indication of an unhealthy environment in East Asia. Environmental Monitoring and Assessment 114, 447—460.

Bierlein, F.P., 1995. Rare-earth element mobility during hydrothermal and metamorphic fluid-rock interaction and the significance of the oxidation state of europium. Chemical Geology 93, 219—230.

Chung, C.-H., 2007. Vegetation response to climate change on Jeju Island, South Korea, during the last deglaciation based on pollen record. Geosciences Journal 11, 147—155.

Davies, B.E., 1980. Applied Soil Trace Elements. Wiley, NewYork, p. 482.

Ding, Z.L., Liu, T.S., Rutter, N.W., Yu, Z.W., Guo, Z.T., Zhu, R.X., 1995. Ice-volume forcing of East Asian winter monsoon variations in the past 800,000 years. Quaternary Research 44, 149—159.

Feng, Q., Endo, K.N., Cheng, G., 2002. Soil carbon in desertified land in relation to site characteristics. Geoderma 106, 21—43.

Gallet, S., Jahn, B.-M., Torii, M., 1996. Geochemical characterization of the Luochuan loess-paleosol sequence, China, and paleoclimatic implications. Chemical Geology 133, 67—88.

Hashizume, M., Ueda, K., Nishiwaki, Y., Michikawa, T., Onozuka, D., 2010. Health effects of Asian dust events: a review of the literature. Japanese Journal of Hygiene 65, 413—421.

Hur, S.D., Lee, J.I., Lee, M.J., Kim, Y., 2003. Determination of rare earth elements abundance in alkaline rocks by inductively coupled plasma mass spectrometry (ICP-MS). Ocean and Polar Research 25, 53—62.

Jaffe, D., Anderson, T., Covert, D., Kotchenruther, R., Trost, B., Danielson, J., Simpson, W., Berntsen, T., Karlsdottir, S., Blake, D., Harris, J., Carmichael, G., Uno, I., 1999. Transport of Asian air pollution to North America. Geophysical Research Letters 26, 711—714.

Janecek, T.R., Rea, D.K., 1983. Eolian deposition in the northwest Pacific Ocean: Cenozoic history of atmospheric circulation. Geological Society of America Bulletin 94, 730—738.

Janecek, T.R., Rea, D.K., 1985. Quaternary fluctuations in the Northern Hemisphere trade winds and westerlies. Quaternary Research 24, 150—163.

Kim, J.C., Lee, Y.I., Lim, H.S., Yi, S., 2012. Geochemistry of Quaternary sediments of the Jeongokri archaeological site, Korea: Implications for provenance and paleoenvironments during the Late Pleistocene. Journal of Quaternary Sciences 27, 260—268.

Kohfeld, K.E., Harrison, S.P., 2003. Glacial-interglacial changes in dust deposition on the Chinese Loess Plateau. Quaternary Science Reviews 22, 1859—1878.

Kwon, H.J., Cho, S.H., Chun, Y., Lagarde, F., Pershagen, G., 2002. Effects of the Asian dust events on daily mortality in Seoul, Korea. Environmental Research 90, 1—5.

Lee, M.W., 1982. Petrology and Geochemistry of Jeju Volcanic Island, Korea. In: Science Report Tohoku University Series III 15, pp. 177—256.

Lee, S.H., Lee, Y.I., Yoon, H.I., Yoo, K.C., 2008. East Asian monsoon variation and climate changes in Jeju Island, Korea during the latest Pleistocene to early Holocene. Quaternary Research 70, 265—274.

Li, C., Yang, S., Zhang, W., 2012. Magnetic properties of sediments from major rivers, aeolian dust, loess soil and desert in China. Journal of Asian Earth Sciences 45, 190—200.

Lim, J., Matsumoto, E., Kitagawa, H., 2005. Eolian quartz flux variations in Cheju Island, Korea during the last 6500 yr and a possible Sun-moon linkage. Quarternary Research 64, 12—20.

Liu, T., Ding, Z., 1998. Chinese loess and the paleomonsoon. Annual Review of Earth and Planetary Sciences 26, 111—145.

Lu, H., Yi, S., Liu, Z., Mason, J.A., Jiang, D., Cheng, J., Stevens, T., Zu, Z., Zhang, E., Jin, L., Zhang, Z., Guo, Z., Wang, Y., Otto-Bliesner, B., 2013. Variation of East Asian monsoon precipitation during the past 21 k.y. and potential CO$_2$ forcing. Geology 41, 1023—1026.

Lu, S.-G., Xue, Q.-F., Zhu, L., Yu, J.-Y., 2008. Mineral magnetic properties of a weathering sequence of soils derived from basalt in eastern China. Catena 73, 23—33.

Maher, B.A., Prospero, J.M., Mackie, D., Gaiero, D., Hesse, P.P., Balkanski, Y., 2010. Global connections between aeolian dust, climate and ocean biogeochemistry at the present day and at the last glacial maximum. Earth Science Reviews 99, 61—97.

McLennan, S.M., Hemming, S., McDaniel, D.K., Hanson, G.N., 1993. Geochemical approaches to sedimentation, provenance, and tectonics. Geological Society of America Special Paper 284, 21—40.

Mizota, C., Endo, H., Um, K.T., Kusakabe, M., Noto, M., Matsuhisa, Y., 1991. The eolian origin of silty mantle in sedentary soils from Korea and Japan. Geoderma 49, 153—164.

Nesbitt, H.W., 1979. Mobility and fractionation of rare earth elements during weathering of a granodiorite. Nature 279, 206—210.

Pausata, F.S.R., Battisti, D.S., Nisancioglu, K.H., Bitz, C.M., 2011. Chinese stalagmite δ^{18}O controlled by changes in the Indian monsoon during a simulated Heinrich event. Nature Geoscience 4, 474—480.

Peterse, F., Prins, M.A., Beets, C.J., Troelstra, S.R., Zheng, H., Gu, Z., Schouten, S., Damsté, J.S.S., 2011. Decoupled warming and monsoon precipitation in East Asia over the last deglaciation. Earth and Planetary Science Letters 301, 256—264.

Pye, K., Zhou, L.P., 1989. Late Pleistocene and Holocene aeolian dust deposition in north China and the northwest Pacific Ocean. Paleogeography Palaeoclimatology Palaeoecology 73, 11—23.

Qiang, M., Liu, Y., Jin, Y., Song, L., Huang, X., Chen, F., 2014. Holocene record of eolian activity from Genggahai Lake, northeastern Qinghai-Tibetan Plateau, China. Geophysical Research Letters 41, 589—595.

Rea, D.K., 1994. The paleoclimatic record provided by eolian deposition in the deep sea: the geologic history of wind. Reviews of Geophysics 32, 159—195.

Rea, D.K., Leinen, M., Janecek, T.R., 1985. Geological approach to the long-term history of atmospheric circulation. Science 227, 721—725.

Ryu, J.S., Lee, K.S., Lee, S.G., Lee, D., Chang, H.W., 2007. Seasonal and spatial variations of rare earth elements in rainwaters, river waters and total suspended particles in air in South Korea. Journal of Alloys and Compounds 437, 344—350.

Shao, Y., Dong, C.H., 2006. A review on East Asian dust storm climate, modelling and monitoring. Global and Planetary Change 52, 1—22.

Sun, J.M., Zhang, M.Y., Liu, T.S., 2001. Spatial and temporal characteristics of dust storms in China and its surrounding regions, 1960—1999: relations to source areas and climate. Journal of Geophysical Research 106, 10325—10333.

Sun, Y., Clemens, S.C., An, Z., Yu, Z., 2006. Astronomical timescale and palaeoclimatic implication of stacked 3.6 Myr monsoon records from the Chinese Loess Plateau. Quaternary Science Reviews 25, 33—48.

VanCuren, R.A., Cahill, T.A., 2002. Asian aerosols in North America: frequency and concentration of fine dust. Journal of Geophysical Research 107 (No. D24), 4804. http://dx.doi.org/10.1029/2002JD002204.

VanCuren, R.A., 2003. Asian aerosols in North America: extracting the chemical composition and mass concentration of the Asian continental aerosol plume from long-term aerosol records in the western United States. Journal of Geophysical Research 108 (No. D20), 4623. http://dx.doi.org/10.1029/2003JD003459.

Wang, Y.J., Cheng, H., Edwards, R.L., An, Z.S., Wu, J.Y., Shen, C.-C., Dorale, J.A., 2001. A high-resolution absolute-dated Late Pleistocene Monsoon record from Hulu Cave, China. Science 294, 2345—2348.

Wang, Y.J., Cheng, H., Edwards, R.L., Kong, S., Shao, S., Chen, S., Wu, J., Jiang, X., Wang, X., An, S., 2008. Millennial- and orbital-scale changes in the East Asian monsoon over the past 224,000 years. Nature 451, 1090—1093.

Wang, X., Sun, D.H., Li, B.F., Wu, S., Guo, F., Li, Z.J., Zhang, Y.B., Chen, F.H., 2013. A high resolution multi-proxy record of late Cenozoic environment change from central Taklamakan Desert, China. Climate of the Past 9, 2731—2739.

Wilde, P., Quinby-Hund, M.S., Erdtmann, B.-D., 1996. The whole-rock cerium anomaly: a potential indicator of eustatic sea-level changes in shales of the anoxic facies. Sedimentary Geology 101, 43—53.

Windom, H.L., 1969. Atmospheric dust records in permanent snowfields: implications to marine sedimentation. Geological Society of America Bulletin 80, 761—782.

Won, J.K., 1976. Study of petrochemistry of volcanic rocks in Jeju Island. Journal of Geological Society of Korea 12, 207—226 (in Korean).

Wright, J., Schrader, H., Holser, W.T., 1987. Paleoredox variations in ancient oceans recorded by rare earth elements in fossil apatite. Geochimica et Cosmochimica Acta 51, 631—644.

Wu, N., Liu, T., Liu, X., Gu, Z., 2002. Mollusk record of millennial climate variability in the Loess Plateau during the Last Glacial Maximum. Boreas 31, 20—27.

Xiao, J.L., Porter, S.C., An, Z.S., Kumai, H., Yoshikawa, S., 1995. Grain size of quartz as an indicator of winter monsoon strength on the Loess Plateau of central China during the last 130,000 yr. Quaternary Research 43, 22—29.

Xiao, J., Inouchi, Y., Kumai, H., Yoshikawa, S., Kondo, Y., Liu, T.S., An, Z.S., 1997. Eolian quartz flux to Lake Biwa, central Japan, over the past 145,000 years. Quaternary Research 48, 48—57.

Xiao, J.L., An, Z.S., Liu, T.S., Inouchi, Y., Kumai, H., Yoshikawa, S., Kondo, Y., 1999. East Asian monsoon variation during the last 130,000 years: evidence from the Loess Plateau of central China and Lake Biwa of Japan. Quaternary Science Reviews 18, 147—157.

Yang, C.Y., Tsai, S.S., Chang, C.C., Ho, S.C., 2005. Effects of Asian dust storm events on daily admissions for asthma in Taipei, Taiwan. Inhalation Toxicology 17, 817—821.

Yang, X., Liu, Y., Li, C., Song, Y., Zhu, H., Jin, X., 2007. Rare earth elements of aeolian deposits in Northern China and their implications for determining the provenance of dust storms in Beijing. Geomorphology 87, 365—377.

Yi, S., Saito, Y., Zhao, Q., Wang, P., 2003. Vegetation and climate changes in the Changjiang (Yangtze River) Delta, China during the past 13,000 years inferred from pollen record. Quaternary Science Reviews 22, 1501—1519.

Zdanowicz, C., Hall, G., Vaive, J., Amelin, Y., Percival, J., Girard, I., Biscaye, P., Bory, A., 2006. Asian dustfall in the St. Elias Mountains, Yukon, Canada. Geochemica et Cosmochimica Acta 70, 3493—3507.

Zhang, X.Y., Arimoto, R., An, Z.S., 1997. Dust emission from Chinese desert sources linked to variations in atmospheric circulation. Journal of Geophysical Research: Atmospheres 102, 28041—28047.

Zhang, X.Y., Arimoto, R., An, Z.S., 1999. Glacial and interglacial patterns for Asian dust transport. Quaternary Science Reviews 18, 811—819.